Rainfall Infiltration and Macropores in a Hillside Slope

AUTHOR(S):

OKA, Taro

CITATION:

OKA, Taro. Rainfall Infiltration and Macropores in a Hillside Slope. Bulletin of the Disaster Prevention Research Institute 1990, 40(1): 1-13

ISSUE DATE:

1990-03

URL:

http://hdl.handle.net/2433/124965

Bull. Disas. Prev. Res. Inst., Kyoto Univ., Vol. 40, Part 1, No. 344, March, 1990

Rainfall Infiltration and Macropores in a Hillside Slope

By Taro Oka

(Manuscript received on January 9, 1990)

Abstract

Infiltration tests and a soil survey made on the slope of a hilly region indicate that the infiltration rate of rainwater decreased rapidly after rain began, that the final infiltration rate was too large for the prevailing soil character, and that coarse macropores occupy 5 to 10% of the horizontal area and fine macropores 7.8% of the volume.

Based on these results, I investigated a numerical simulation model of rainfall infiltration in a hillside slope. First, the amount of rainfall infiltrating soil containing fine macropores was calculated from a model that combined viscous flow within the capillary tubes and unsaturated soil water flow. These calculations showed that fine macropores increase the hydraulic conductivity of the soil 5– to 10–fold. Next, the amount of rainfall infiltrating soil containing coarse macropores was calculated based on the following assumptions: (a) The coarse macropores were filled with coarse, porous material of high hydraulic conductivity. (b) The soil around these coarse macropores was uniform and homogeneous. (c) To take into account the effects of fine macropores, the hydraulic conductivity was set 5 times larger than the observed hydraulic conductivity of the soil. The calculated results agree well with the infiltration curves obtained from field tests.

1. Introduction

The presence of large continuous openings (macropores), such as cracks and holes caused by desiccation, tiny animals in the soil and the rotting of roots, affects the infiltration of rainwater to soil.

Beven and Germann[1] (1982) have reviewed recent studies of macropores. Furthermore, in their analysis of rainfall infiltration to soil containing macropores, Germann and Beven [2] (1985) presented a two-domain flow model in which the flow in macropores is expressed by the kinematic wave theory and the flow in the soil by Philip's sorptivity concept. In addition, Beven and Clarke[3] (1986) have reported a method with which to analyze rainwater infiltration into a homogeneous soil matrix containing a population of macropores. In that model, having neglected the flow-down time in the macropores, they described the flow in the soil by the Green and Ampt model.

Although the study of the infiltration of rainwater into soil containing macropores has progressed, no simplified theoretical analysis can explain it fully because of the complexity of the soil structure on slopes in hilly regions.

I have carried out an infiltration test to better understand rainfall infiltration phenomena in a naturally hilly region. Having then divided the macropores into coarse and fine categories, I measured the distributions of these macropores. In the third part, I have developed a numerical simulation model that expresses the rainfall infiltration

process into soil containing macropores, based on previous experimental results.

2. Measurements of the Rainwater Infiltration Rate on a Slope in a Hilly Region

The infiltration rate was measured with an apparatus such as shown in **Fig. 1.** The apparatus is comprised of artificial rainfall generation equipment, a water supplier, and a measurement device. The artificial rainfall generation equipment is a container with 100 cm longitudinal and transverse lengths and 3 cm in height, and hypodermic needle shaped nozzles are embedded at 5 cm intervals on the bottom of the container. Homogeneous rainfalls of more than 30 mm/h can be generated by reducing the pressure within the container to negative by lowering a constant head tank. The water supplier is comprised of lower tank → pump → flow rate control valve (Vp) → constant head tank → artificial rain generation equipment. The flow rate control valve has a function to adjust flow rate and to maintain it at a constant rate during the infiltration test. The measurement of rainfall is made by using a tipping bucket rain gauge. The surface flow is collected downstream of the experimental plot and is also measured utilizing the flow rate gauge of a tipping bucket type. The infiltration from the soil surface can be calculated from the difference between the rainfall and the surface runoff.

At point A in the basin of the Tanida River, in the west of Kyoto City (**Fig. 2**), I measured the infiltration rate. The experimental plot was 1.0 m long, 0.315 m wide and had a 52% slope. The surface soil of the plot, which is covered to a depth of 1 to 2 cm by fallen bamboo leaves and humus, is clay, and its saturated hydraulic conductivity is 4.5 mm/h.

The infiltration rates obtained are shown in **Fig. 3.** The rate decreases rapidly once rainfall has begun, and 7 min later it converges asymptotically to an almost constant value of 55 mm/h. Thus, the infiltration rate on a slope in a hilly region is far larger

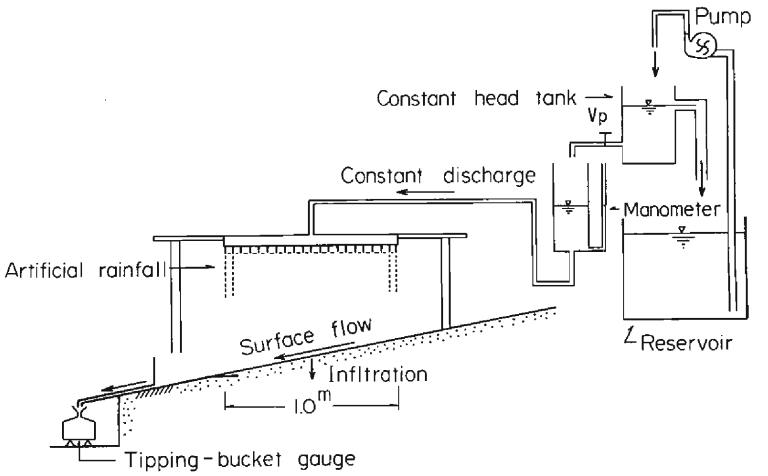

Fig. 1. Schematic illustration of the infiltration test equipment.

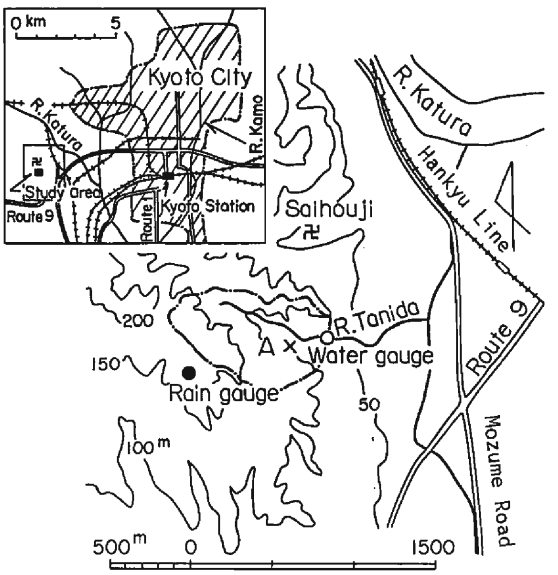

Fig. 2. Physiographical map of Tanida research basin.

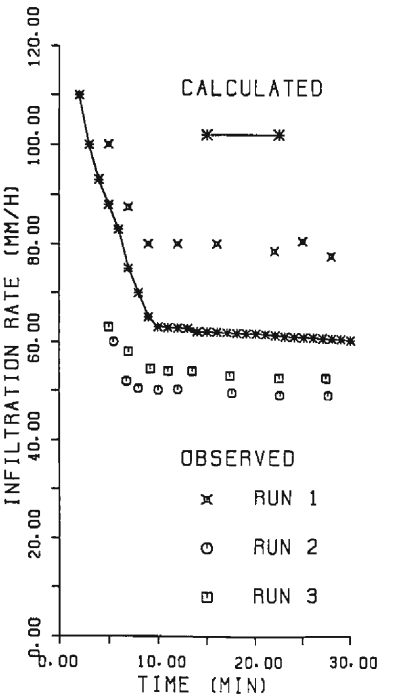

Fig. 3. Infiltration rates measured at plot A.

than the value derived from the saturated hydraulic conductivity of the surface soil. Removal of the layer of dead leaves after a series of experiments brought to light macropores which are thought to have been caused by root-rot. I concluded that almost all the rainwater that reaches the slope enters these macropores, thereby increasing the rate of infiltration.

3. Macropore Measurements

The classification and naming of pore-types present in a soil have been discussed by scientists, but there has been no general agreement on them. I have roughly divided pores into two types; matrix pores produced by the contact of soil particles, and macropores formed by desiccation, animals in the soil, root-rot, etc. I also have subdivided macropores into coarse macropores, whose shapes and distributions can be determined visually, and fine macropores which cannot be measured visually. Although not all researchers agree on the classification of pores by macropore size, for my purposes I have called macropores that have diameters greater than 5 mm, coarse macropores, and those that have diameters less than 5 mm, fine macropores. Macropores present on slopes in hilly regions vary greatly and include bare holes and pores that are partly or completely filled with dead leaves and humus. Although coarse macropores filled with

dead leaves are no longer macropores in the strict sense, I have included them in this group because they are considered holes when generated.

3.1 Coarse macropore Measurements

Methods with which to measure the distribution of macropores (Bouma et al.[4] (1982), Petrovic et al.[5] (1982)) have been reported, but I have chosen the primitive but assured method of visual observation. After removal of the dead leaves and humus from the soil surface, I measured the horizontal distribution of the coarse macropores by tracing them on a transparent plastic board. Vertical distribution was measured by digging a hole and drawing a sketch of its wall surface. The distribution of coarse macropores around the infiltration test plot is shown in **Fig. 4**. Only large, hole-shaped pores with diameters greater than several centimeters are shown because those of smaller diameter could not be measured after the disarrangement of the soil surface caused by the removal of the dead leaf layer. These holes are mainly the result of the root-rot of bamboo, and almost all are filled with dead leaves or humus. The ratio of the coarse macropores to the test area is 5 to 10%.

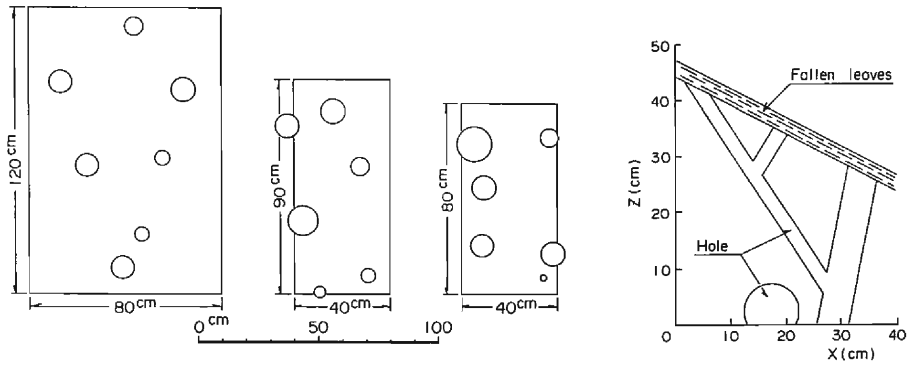

(a) Horizontal distributions. (b) Vertical distributions.

Fig. 4. Distributions of coarse macropores.

3.2 Fine macropore Measurements

It is not easy to measure the distribution of fine macropores in naturally hilly regions because of their small size. I investigated the fine macropores as follows: (a) Porosity was measured by sampling with a small soil sampler driven into the plot at a place where no macropores were present. The sampler had an inside diameter of 4.3 cm and a length of 5.0 cm. This porosity should be regarded only as a consequence of the matrix pore. (b) Porosity was measured by sampling soil in an area with a radius of about 15 cm and depth of 20 cm, in which no coarse macropores were present. Knowing the volume of the sampled soil is indispensable for the measurement of porosity. The sand-replace method was used, in which the hole from which the soil had been taken was filled with sand of a known weight per unit volume. The volume of the sample

taken could be calculated from the weight of this sand.

Results of porosity measurements made around the infiltration plot are shown in **Fig. 5.** The average porosity obtained with the small sampler is 0.550 and that of the porosity in the larger area, 0.628, the difference being 0.078. Consequently, fine macropores make up 7.8% of the volume.

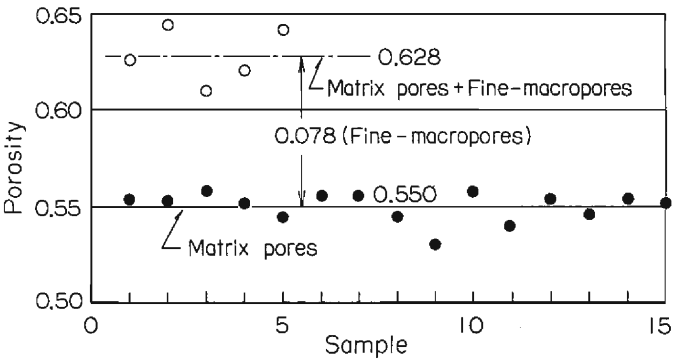

Fig. 5. Porosities measured in the Tanida River basin.

4. Rainfall infiltration Analysis of Soil with Macropores

Analysis of soil water movement in soil containing both fine and coarse macropores is necessary to clarify the rainfall infiltration mechanisms on a slope of a hilly region. However, it is difficult to consider both simultaneously in a numerical analysis because of the difference in size. I have determined rainfall infiltration on a slope in a hilly region using a three step analysis:

4.1 Rainfall infiltration analysis of soil with fine macropores

(1) Numerical simulation model

Soil water flow in soil that does not contain macropores is expressed by Richards' Equation (1).

$$C(\theta)\frac{\partial \Psi}{\partial t}=\frac{\partial}{\partial x}\left[K(\theta)\frac{\partial \Psi}{\partial x}\right]+\frac{\partial}{\partial z}\left[K(\theta)\left(\frac{\partial \Psi}{\partial z}+1\right)\right] \tag{1}$$

Here Ψ is the pressure head; in which $\Psi \geq 0$ in a saturated domain and $\Psi < 0$ in an unsaturated domain. $K(\theta)$ is the unsaturated hydraulic conductivity when θ is the volumetric moisture content, $C(\theta)$ the specific moisture capacity, x the horizontal coordinate, z the vertical coordinate and t the time.

Although flow through fine macropores can be regarded as viscous flow in a capillary tube, it is difficult to treat it as such in the strict sense. Therefore, it should be assumed to be equivalent to the unsaturated soil water flow. Using this assumption, both the flow in fine macropores and the unsaturated soil water flow in the soil can be analyzed

simultaneously with Eq. (1). Eq. (1) can be solved by the Galerkin finite element method (Neuman[6] (1973)).

It is necessary to know beforehand values for $\Psi(\theta)$ and $K(\theta)$ that correspond to fine macropores, which can be ascertained as follows: Rainwater in fine macropores is regarded as a viscous flow in a capillary tube with a radius of r cm. The saturated hydraulic conductivity, $K_{sat.}$, is calculated from Eq. (2), derived from the Hagen-Pousuelle Law and the height of the capillary rise, h_t, from Eq. (3).

$$K_{sat.}=r^2g\rho/8\mu \tag{2}$$

$$h_t=2\sigma\cos\alpha/r\rho g \tag{3}$$

g: acceleration of gravity, ρ: density, μ: viscosity, σ: the surface tension coefficient; α: the contact angle ($\alpha=0.0$). For example, when $r=0.05$ cm, $K_{sat.}=27.8$ cm/s and $h_t=2.98$ cm. Using these $K_{sat.}$ and h_t values, the $\Psi(\theta)$ and $K(\theta)$ of the fine macropores can be estimated by Equations (4) and (5) adopted by Pikul, Street and Remson[7] (1974).

$$\frac{\theta-\theta_r}{\theta_0-\theta_r}=\frac{a}{[a+c(-\Psi)^b]} \tag{4}$$

$$\frac{K(\theta)}{K_{sat}}=\left[\frac{a}{[a+c(-\Psi)^b]}\right]^N \tag{5}$$

θ_0 : saturated soil moisture content, r : residual soil moisture content, a, b, c, N : soil parameters.

(2) Analysis conditions

Measurements of fine macropores in the surface soil of the basin of the Tanida River showed a 7.8% volume ratio. As the actual distribution and shapes of the fine macropores have not yet been determined, it was assumed that fissures 0.1 cm wide and 5 cm deep were distributed in parallel at 1.5 cm intervals, (**Fig. 6**). When the above configuration for the analysis section is assumed, it is sufficient to analyze only half the A-A section shown in **Fig. 6** because of the symmetry of flow. The analysis section and element division used in the calculations are shown in **Fig. 7.** A 1-cm-deep layer of dead leaves with large hydraulic conductivity covers the upper part of the analysis site.

Boundary conditions to solve Eq. (1) are as follows: On the soil surface, when the amount of precipitation is given

$$q=-R. \tag{6}$$

q: the normal flux per unit length of boundary, R: rainfall intensity. When the soil surface is saturated,

$$\Psi=0. \tag{7}$$

On an impervious layer or symmetrical surface,

$$q=0. \tag{8}$$

$\Psi(\theta)$ and $K(\theta)$, which correspond to the fine macropores, are calculated by substituting $K_{sat.}=27.8$ cm/s, $a=30.0$, $b=2.0$, $c=0.01$, $\theta_0=1.0$, $\theta_r=0.0$, and $N=2$ in Eqs. (4) and (5).

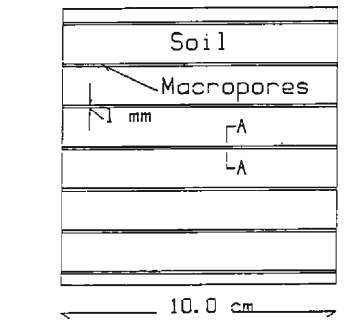

(a) Horizontal section.

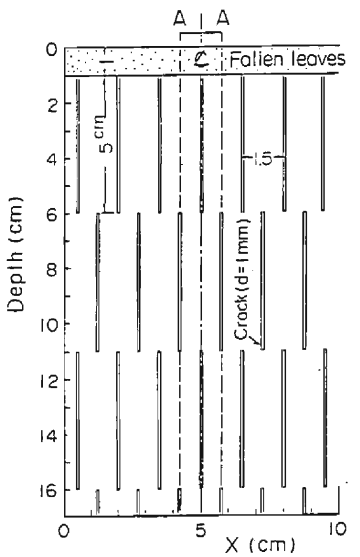

(b) Vertical section.

Fig. 6. Distribution model of fine macropores.

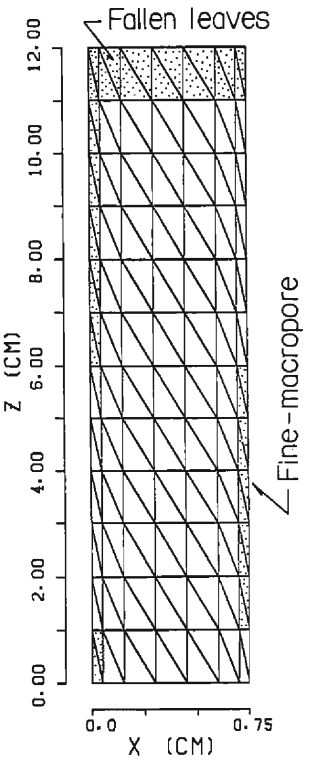

Fig. 7. Finite element meshes used to calculate the soil water flow in fine macropores and soil.

$\Psi(\theta)$ and $K(\theta)$, which correspond to the soil around the fine macropores, are shown in **Fig. 8**. These were measurd in an indoor experiment for the surface soil in the basin of the Tanida River.

The values Ψ_a and K_a in **Fig. 12** are used as the $\Psi(\theta)$ and $K(\theta)$ of the dead leaf layer at the top of the analysis section. Furthermore, although Ψ_a and K_a have been measured in sandy soil, they have almost the same coefficient as the dead leaf layer.

Other analysis conditions were the time increment $\Delta t = 0.001$ sec and $R = 100$ mm/h. The initial value for the dead leaves layer, $\Psi = -10$ cmH_2O has been assumed, otherwise $\Psi = -100$ cmH_2O is used.

(3) Calculation results

The vectors of velocity and pressure distributions at $t = 10$ sec and 20 sec derived

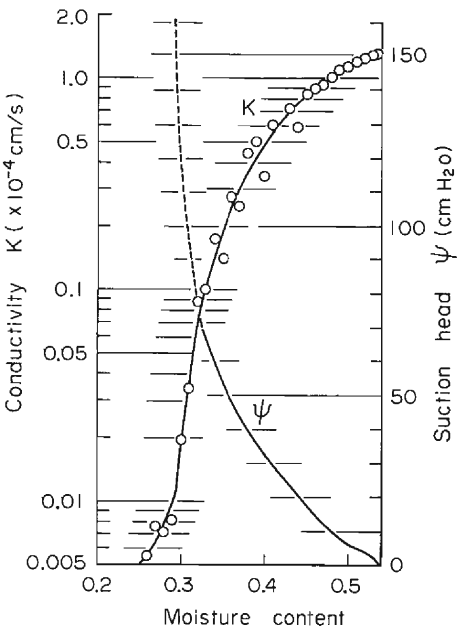

Fig. 8. $\Psi(\theta)$ and $K(\theta)$ of the surface soil in Tanida River basin.

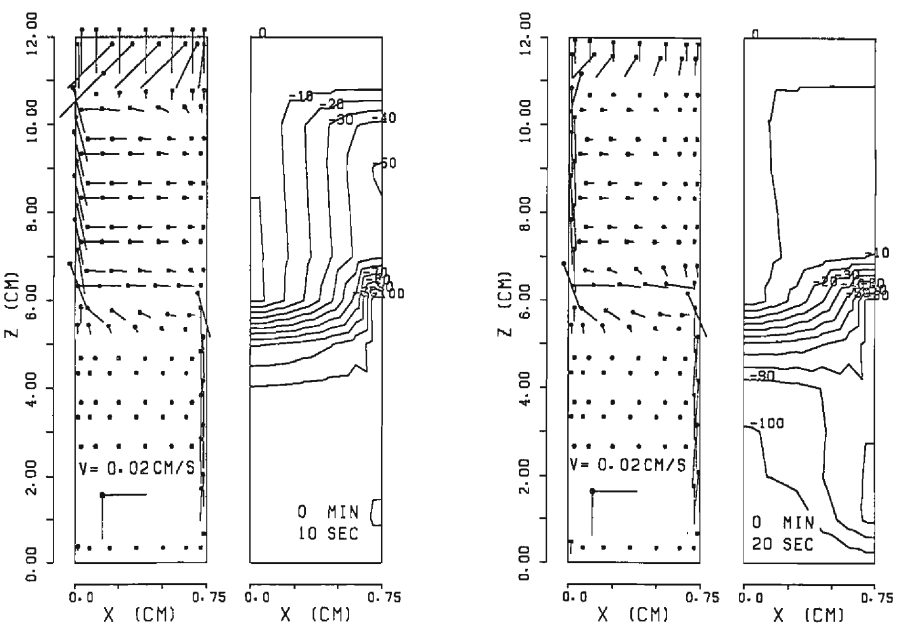

Fig. 9. Velocity vector and pressure head in fine macropores and soil.

from the calculations, are shown in **Fig. 9**, in which a velocity of flow larger than V_x, V_z >0.02 cm/s is represented as V_x, $V_z=0.02$ cm/s. In this calculation, the bottoms of the fine macropores at the top of the section are saturated about 9 sec later after rain has begun, and these are filled with water about 17 sec later.

At $t=10$ sec (**Fig. 9**), rainwater infiltrates the fine macropores on the left side of the section after passing through the dead leaf layer and descends at a high velocity inside these macropores. Rainwater infiltration into the nearby soil from the surface and fine macropores also takes place. At $t=20$ sec, the domain 6 cm below the soil surface is almost saturated and the velocity of flow decreases, at which time infiltration of the fine macropores on the right side begins. Thus, in soil containing fine macropores, rainwater descends through the fine macropores → soil → fine macropores route. Therefore, fine macropores have the effect of making the infiltration of rainwater faster.

4.2 Vertical one-dimensional analysis and simplification of the analysis of rainwater infiltration of soil containing fine macropores

The model of rainwater infiltration of soil containing fine macropores shown here requires numerous calculations, and is not practical in terms of cost. Therefore simplification of the rainfall infiltration analysis using one-dimensional analysis was investigated.

Soil moisture distribution after 10 sec obtained by setting $K(\theta)$ equal to, 5 times and 10 times the values in **Fig. 8**, are shown as K, $K*5$, and $K*10$ in **Fig. 10.** In this figure, the soil moisture distribution shown by FM, is obtained by averaging the soil moisture distributions in the horizontal direction according to the two-dimensional model.

A comparison of K and FM in **Fig. 10**, shows that the wetting front of FM is 6 cm deep, whereas the wetting front of K is 1.5 cm deep, a marked difference in values.

A comparison of $K*5$, $K*10$ and FM shows that the wetting front of $K*5$ is about 3 cm deep and that of $K*10$ about 4 cm deep. The soil moisture distribution of $K*10$ ap-

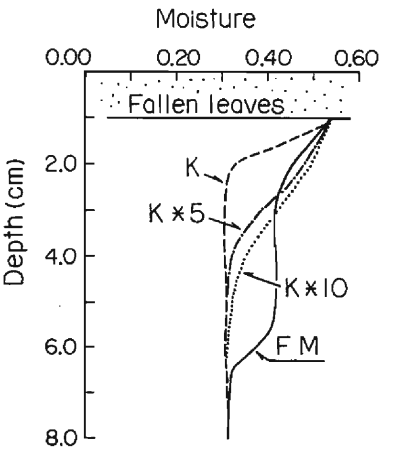

Fig. 10. Comparison of soil moisture distributions calculated by the two-dimension model (FM) and one-dimensional models (K, $K*5$, $K*10$).

proaches that of FM. I, therefore, concluded that a vertical, one-dimensional analysis can approximate the actual rainfall infiltration of soil that contains fine macropores if the unsaturated hydraulic conductivity value is increased by a factor of 10.

4.3 Analysis of rainwater infiltration of soil containing coarse macropores

(1) Analysis model

The infiltration of rainwater into soil containing coarse macropores was analyzed with the following model. Although coarse macropores are three dimensional, they have been treated as two dimensional to maintain the ratio between them and the soil surface area. Coarse macropores may be empty, but here they are considered as being filled with humus. Fine macropores are neglected, and the soil is assumed to be uniform and homogeneous. To include the effect of fine macropores, the $K(\theta)$ of the soil must be set 5 to 10 times larger than the actual unsaturated hydraulic conductivity.

In this model, the slope in a hilly region consists of two kinds of permeable layers with different conductivity. Consequently, the infiltration of rainwater can be analyzed by applying Richards' equation as was done for the fine macropores.

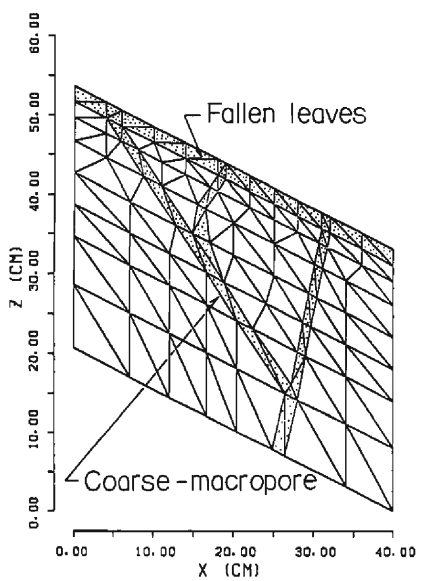

Fig. 11. Finite element meshes used to calculate the soil water flow in the coarse macropores and soil.

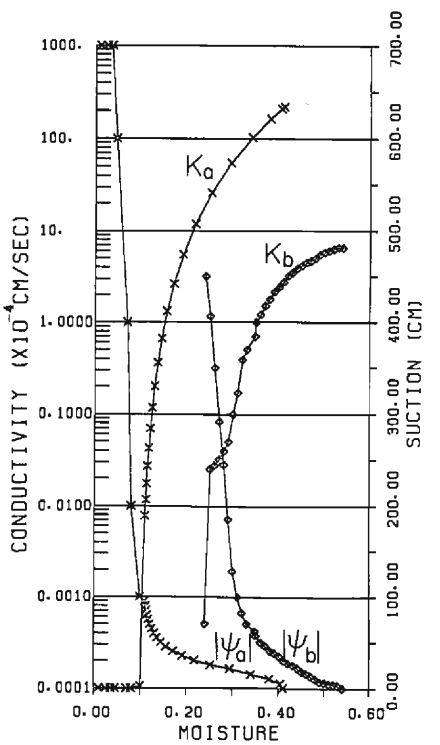

Fig. 12. $\Psi(\theta)$ and $K(\theta)$ for the dead leaf layer and soil containing fine macropores.

(2) Analysis conditions

The analysis section is assumed (**Fig. 11**), to refer to the distribution of the coarse macropores shown in **Fig. 4.** Three coarse macropores are present under the dead leaf layer on this analysis plane, the areal ratio for macropores being 10%. The element divisions used for analysis are presented in **Fig. 11.**

Values of $\Psi(\theta)$ and $K(\theta)$ for the dead leaf layer and the plugs in the macropores are shown in **Fig. 12** (Ψ_a, K_a). The hydraulic conductivity of soil containing fine macropores, first was set 10 times larger than the value shown in **Fig. 8.** The calculated infiltration rate, however, was too large when compared with the measured value shown in **Fig. 3**; therefore, the $K(\theta)$ of the soil containing fine macropores was set 5 times larger. Because fine macropores have little effect on $\Psi(\theta)$, it stays invariant. (Cf. **Fig. 12** (K_b, Ψ_b))

The boundary and initial conditions were similar to those for the fine macropores. Because the soil surface is inclined, the downstream end of the dead leaf layer is considered a seepage face. Other conditions; Rainfall intensity $R=100$ mm/h, and the time increment $\Delta t=10$ sec.

(3) Calculation results

The vector of velocity and the pressure distribution derived from the calculations

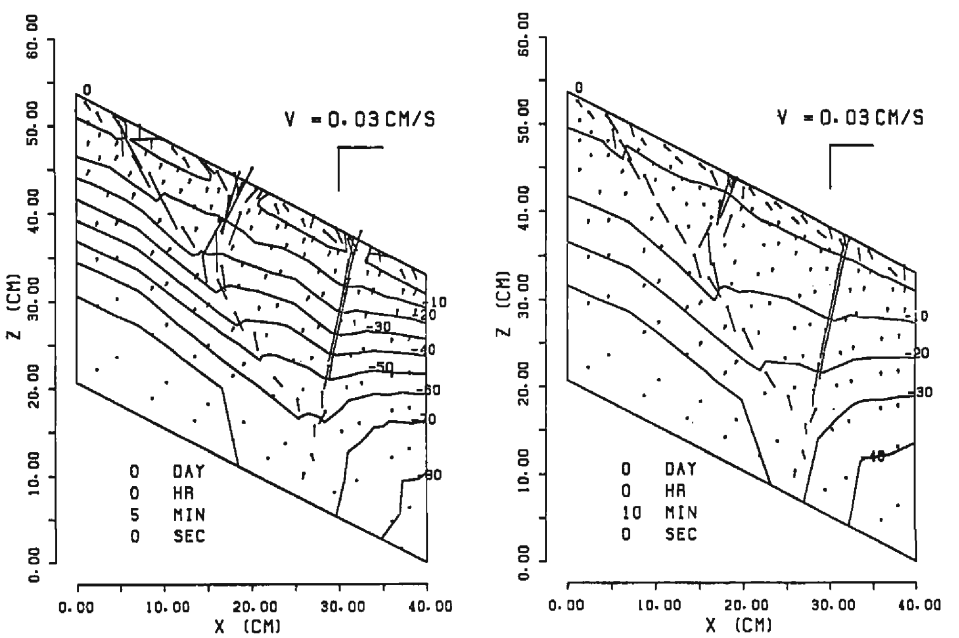

(a) $t=5$ min. (b) $t=10$ min.

Fig. 13. Velocity and pressure head in coarse macropores and soil.

are shown in **Fig. 13**. Based on the velocity distribution, rainwater infiltrates the dead leaf layer in the downstream direction after reaching the soil surface, then changes direction at the upper part of the coarse macropores and flows into them, where it descends with high velocity and infiltrates from the wall surface into the soil.

Infiltration rates derived from the calculations are shown in **Fig. 3**. The calculated rates agree well with the results of the infiltration tests.

5. Conclusions

To clarify the rainfall infiltration mechanism that operates on a slope in a naturally hilly region, I conducted infiltration tests, a soil survey and rainfall infiltration analyses. Although the composition of the soil in hilly regions is very complicated and various factors have still to be accounted for, the rainfall infiltration mechanism that operates on slopes has now been fairly well clarified by my experimental and calculated analyses:

(1) The rainfall infiltration rate on a slope in naturally hilly regions is far larger than the value derived from the saturated hydraulic conductivity of the surface soil. The rainfall infiltration rate decreases rapidly after rain begins.

(2) Macropores that have been created by desiccation, tiny animals in the soil and the rotting of roots are present in naturally hilly regions. These macropores were classified into two groups; fine and coarse macropores. In the surface soil of the Tanida River basin, fine macropores account for 7.8% of the total volume and coarse macropores for 5 to 10% of the surface area.

(3) Results of the analysis of rainwater infiltration into the soil containing fine macropores show that almost the entire volume of a rainfall descends through the soil, taiking the route fine macropores (vertical) → soil (horizontal) → fine macropores (vertical). Macroscopically, the fine macropores speed up rainwater infiltration.

(4) By setting the unsaturated hydraulic conductivity 5 to 10 times larger than the measured value, a one-dimensional analysis gives a close approximation of the actual rainfall infiltration of soil that contains fine macropores.

(5) On slopes containing coarse macropores, almost all the rainwater flows into them and descends at a high velocity. At the same time, it infiltrates the soil through the wall surface of the coarse macropores. Thus, on slopes with coarse macropores, the movement of soil moisture is increased.

(6) Results of calculations of the infiltration rate of rainwater in soil containing coarse macropores agree well with infiltration curves obtained in the field. Consequently, this method for analysing the rainwater infiltration of slopes in hilly regions is a usuful one.

References

1) Beven, K. J. and P. Germann: Macropores and Water Flow in Soil, Water Resour. Res., Vol. 18, No. 5, 1982, pp. 1311–1325.

2) Germann, P. F. and Beven, K. J.: Kinematic Wave Approximation to Infiltration into Soils with Sorbing Macropores, Water Resour. Res., Vol. 21, No. 7, 1985, pp. 990–996.
3) Beven, K. J. and R. T. Clarke: On the Variation of Infiltration into a Homogenous Soil Matrix Containing a Population of Macropores. Water Resour. Res., Vol. 22, No. 3, 1986, pp. 383–388.
4) Bouma, J., C. F. M. Belmans, and L. W. Dekker: Water Infiltration and Redistribution in a Silt Loam Subsoil with Vertical Worm Channels, Soil Sci. Soc. Am. J., Vol. 46, No. 5, 1982, pp. 917–921.
5) Petrovic, A. M., J. E. Siebert and P. E. Rieke: Soil Bulk Density Analysis in Three Dimensions by Computed Tomographic Scanning, Soil Sci. Soc. Am. J., Vol. 46, No. 3, 1982, pp. 445–450.
6) Neuman, S. P.: Saturated-Unsaturated Seepage by Finite Elements, Proc. of Am. Soc. Civ. Eng. Vol. 99, No. HY12, 1973, pp. 2233–2250.
7) Pikul, M. F., R. L. Street and I. Remson: A Numerical Method Based on Coupled One-Dimensional Richards and Boussinesq Equations, Water Resour. Res. Vol. 10, No. 2, 1974, pp. 295–302.

A part of this paper has been published in the Post-Conference Proceeding of International Conference on Infiltration Development and Application, Water Resources Research Center, University of Hawaii at Manowa, 1988.